
On Convergence of Nearest Neighbor Classifiers over Feature Transformations

Luka Rimanic*

ETH Zurich

luka.rimanic@inf.ethz.ch

Cedric Renggli*

ETH Zurich

cedric.renggli@inf.ethz.ch

Bo Li

UIUC

lbo@illinois.edu

Ce Zhang

ETH Zurich

ce.zhang@inf.ethz.ch

Abstract

The k-Nearest Neighbors (kNN) classifier is a fundamental non-parametric machine learning algorithm. However, it is well known that it suffers from the *curse of dimensionality*, which is why in practice one often applies a kNN classifier on top of a (pre-trained) feature transformation. From a theoretical perspective, most, if not all theoretical results aimed at understanding the kNN classifier are derived for the *raw* feature space. This leads to an emerging gap between our theoretical understanding of kNN and its practical applications.

In this paper, we take a first step towards bridging this gap. We provide a novel analysis on the convergence rates of a kNN classifier over transformed features. This analysis requires in-depth understanding of the properties that connect *both* the transformed space and the raw feature space. More precisely, we build our convergence bound upon two key properties of the transformed space: (1) *safety* – how well can one recover the raw posterior from the transformed space, and (2) *smoothness* – how complex this recovery function is. Based on our result, we are able to explain why some (pre-trained) feature transformations are better suited for a kNN classifier than others. We empirically validate that both properties have an impact on the kNN convergence on 30 feature transformations with 6 benchmark datasets spanning from the vision to the text domain.

1 Introduction

The k-Nearest Neighbor (kNN) algorithms form a simple and intuitive class of non-parametric methods in pattern recognition. A kNN classifier assigns a label to an unseen point based on its k closest neighbors from the training set using the maximal vote [1]. Even its simplest form, the 1NN classifier, converges to an error rate that is at most twice the *Bayes error* – the *minimal* error of any classifier [10]. Furthermore, when $k = k_n$ is a sequence satisfying $k_n/n \rightarrow 0$, as $n \rightarrow \infty$, the kNN classifier is consistent, meaning that its error converges to the Bayes error almost surely [34]. In recent times, kNN algorithms are popular, most often due to their simplicity and valuable properties that go beyond accuracy: (a) evaluation of Shapley value in polynomial time, used to outperform a range of other data valuation algorithms, whilst being orders of magnitude faster [19, 20, 21]; (b) estimation of the Bayes error [10, 12, 33]; (c) robustness analysis [28, 39]; (d) efficiency in enabling tools such as provable robust defenses [41]; (e) polynomial-time evaluation of the exact expectation of kNN over a tuple-independent database [24], which is generally hard for other classifiers; (f) applications to conformal inference tasks benefit from the fact that no training is required for running kNN [30].

*Equal contribution.

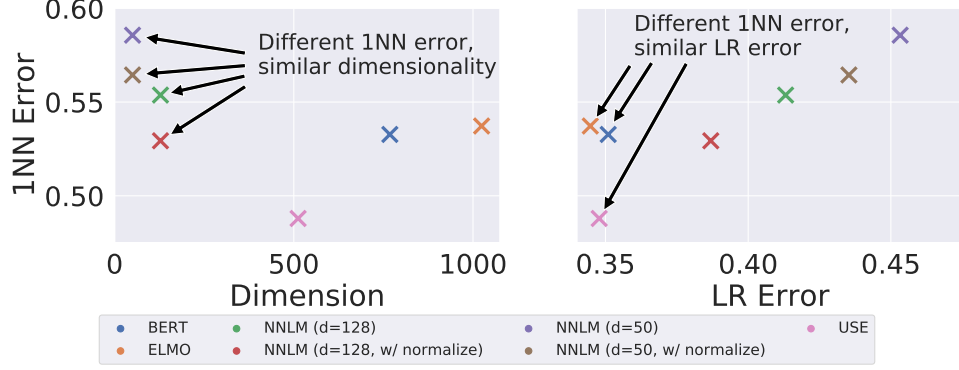


Figure 1: Challenges of examining the behavior of the 1NN classifier on top of feature transformations on YELP dataset. **(Left)** 1NN vs. dimension, **(Right)** 1NN vs. LR Error.

However, being itself a simple classifier, most of the above applications require kNN to be run on top of a feature transformation, ranging from simpler ones, such as PCA, to more complex transformations, such as neural networks pre-trained on another task.

At the same time, most, if not all, theoretical results on kNN are derived under assumptions that the algorithms are directly applied on the raw data, resulting in an *emerging gap between the theoretical understanding of kNN and its practical applications*. In this paper we take a step towards closing this gap. Specifically, we are interested in the *convergence behavior* of kNN over transformations: *Given a transformation f and a set of n training examples, can we describe the (expected) error of kNN over f as a function of n and some properties of the transformation f ?* In other words, given a fixed n , what are the properties of f that strongly correlate with the kNN error over f ?

Challenges. Giving an informative answer to these questions is nontrivial as many simple, intuitive hypothesis alone cannot fully explain the empirical behavior of kNN over feature transformations.

First, as many existing results on the convergence have a factor of $(k/n)^{1/D}$, where D is the dimension of the space, a natural hypothesis could be: *given a fixed n , transformations resulting in lower D have lower kNN error*. While this is plausible, it leaves many empirical phenomena unexplained. For example, Figure 1 (left) illustrates kNN errors over feature transformations with different dimensions, showing a real-world dataset in which transformations of the same dimension have drastically different kNN accuracies. Another approach is to consider the *accuracy* of some other classifier. For example, training a logistic regression (LR) model on f and using it directly to form a hypothesis: *given a fixed n , transformations that lead to higher logistic regression accuracy have lower kNN error*. This is a much stronger hypothesis and can explain many scenarios that dimensionality alone cannot. However, Figure 1 (right) shows that this still leaves some important cases unexplained, providing examples in which multiple transformations achieve similar logistic regression accuracies, whilst having noticeably different kNN accuracies.

Summary of Results and Contributions. In this paper we take a step towards understanding the behavior of a kNN classifier over feature transformations. As one of the first papers in this direction, our results by no means provide the *full* understanding of *all* empirical observations. However, we provide a novel theoretical understanding that explains more examples than the above notions and hope that it can inspire future research in this direction. Our key insight is that the behavior of kNN over a feature transformation f relies on two key factors: (1) *safety* – how well can we recover the posterior in the original space from the feature space, and (2) *smoothness* – how hard it is to recover the posterior in the original space from the feature space?

We answer these two questions by defining and examining *safety* as the decrease in the best possible accuracy of any classifier (i.e., the Bayes error) in the feature space when compared to the original features, whilst we use the geometrical nature of the transformed features to examine *smoothness*.

More precisely, let \mathcal{X} be the feature space and \mathcal{Y} the label space. In line with previous work on convergence rates of a kNN classifier, throughout the theoretical analysis we restrict ourselves to binary classification with $\mathcal{Y} = \{0, 1\}$. For random variables X, Y that take values in \mathcal{X}, \mathcal{Y} and are jointly distributed by $p(x, y) = p(X=x, Y=y)$, let $\eta(X) = p(1|X)$ be the true posterior probability.

The main task is to recover $\eta(X)$ by $(g \circ f)(X)$, where g is a trainable function for a fixed architecture, and f is a feature transformation. We show that the above notions can be accordingly bounded by a function involving the L^2 -error defined by $\mathcal{L}_{g,X}(f) = \mathbb{E}_X((g \circ f)(X) - \eta(X))^2$, and L_g , a Lipschitz constant of g . In particular, we prove that the convergence rate of a kNN classifier over a feature transformation f is upper bounded by $\mathcal{O}(1/\sqrt{k} + L_g \sqrt[4]{k/n} + \sqrt[4]{\mathcal{L}_{g,X}(f)})$. The result depicts a trade-off between the safety of a feature transformation, represented by $\mathcal{L}_{g,X}(f)$, and the smoothness, represented by L_g . For example, the most common implementation of transfer learning is given by $g(x) = \sigma(\langle w, x \rangle)$, where σ is the sigmoid function, in which case one can take $L_g = \|w\|_2$. We show that with this formulation we can explain the relative performance of many transformations used in the kNN setting. An important insight one might take is the following: *For two transformations that have similar $\mathcal{L}_{g,X}(f)$, the one with smaller $\|w\|_2$ will likely achieve better performance with respect to a kNN classifier.*

We highlight the usefulness and validate our novel theoretical understanding by conducting a thorough experimental evaluation ranging over 6 real-world datasets from two popular machine learning modalities, and 30 different feature transformations.

2 Related Work

As one of the fundamental machine learning models, the kNN classifier enjoy a long history of theoretical understanding and analysis. The first convergence rates of a kNN classifier were established in [9], where convergence rates of 1NN in \mathbb{R} under the assumption of uniformly bounded third derivatives of conditional class probabilities were given, further extended to \mathbb{R}^d in [14, 38]. Distribution-dependant rates of convergence have been examined in [17, 26], where certain smoothness assumptions were imposed. These were further developed in [7] through the notion of effective boundary, similar to the margin and strong density conditions examined in [3, 13, 15, 25, 37]. Finally, [18] provides convergence rates under the simplest assumptions, which perfectly suit our purposes. To the best of our knowledge, all previous works on the rates of convergence of kNN classifiers are derived on raw features. The goal of this work is to understand the convergence of kNN classifiers on transformed features, an emerging paradigm that we believe is, and will be, of great importance in practice.

It is no secret that kNN classifiers over raw features are cursed, suffering from what is known as the *curse of dimensionality* [10, 32, 33]. In practice, there have been many results that apply kNN classifiers over feature transformations. In the easiest form, such transformations can be as simple as a PCA transformation [23, 27, 36]. Recently, a popular choice is to apply kNN over pre-trained deep neural networks [4, 19, 28, 40]. Other related works propose to optimize a neural feature extractor explicitly for a kNN classifier [16, 42]. Most of these results show significant improvements on accuracy, empirically, bringing the performance of a simple kNN classifier on a par with state-of-the-art models. However, there is an obvious lack of rigorous understanding of properties that a feature transformation needs to satisfy in order to achieve a good kNN performance. This work is inspired by the empirical success of applying kNN on transformed features with the aim of providing the first theoretical analysis of kNN over feature transformation.

3 Preliminaries

For a training set $\mathcal{D}_n := \{(x_i, y_i)\}_{i \in [n]}$, and a new instance x , let $(x_{\pi(1)}, \dots, x_{\pi(n)})$ be a reordering of the training instances with respect to their distance from x , through some appropriate metric. In that setting, the *kNN classifier* $h_{n,k}$ and its *n-sample error rate* are defined by

$$h_{n,k}(x) = \arg \max_{y \in \mathcal{Y}} \sum_{i=1}^k \mathbf{1}_{\{y_{\pi(i)}=y\}}, \quad (R_X)_{n,k} = \mathbb{E}_{X,Y} \mathbf{1}_{\{h_{n,k}(X) \neq Y\}},$$

respectively. The *infinite-sample error rate* of kNN is given by $(R_X)_{\infty,k} = \lim_{n \rightarrow \infty} (R_X)_{n,k}$.

Bayes error rate (BER), the error rate of the *Bayes optimal classifier*, often plays a central role in the analysis of kNN classifiers [7, 13, 18]. It is the lowest error rate among all possible classifiers from \mathcal{X} to \mathcal{Y} , and can be expressed as

$$R_{X,Y}^* = \mathbb{E}_X [1 - \max_{y \in \mathcal{Y}} \eta_y(x)],$$

which we abbreviate to R_X^* when Y is obvious from the context. Under applying certain transformation $f: \mathcal{X} \rightarrow \tilde{\mathcal{X}}$, we denote the BER in $\tilde{\mathcal{X}}$ by $R_{f(X)}^*$, and further define $\Delta_{f,X}^* = R_{f(X)}^* - R_X^*$.

4 Impact of Transformations on kNN Convergence

The main goal of this section is to provide a novel theoretical guarantee on the behavior of convergence rates of a kNN classifier over feature transformations. We state the main ingredients and show how they are used to prove the main theorem, whilst the proofs for these ingredients can be found in Section A of the supplementary material, in the same order as presented here.

Overview of Results. We begin by providing an overview of our results before expanding them in details in the next two sections.

It is well known that a kNN classifier can converge arbitrarily slowly if one does not assume any regularity [2]. A common starting assumption for determining convergence rates of a kNN classifier is that of the a-posteriori probability $\eta(x)$ being an L -Lipschitz function, that is for all $x, x' \in \mathcal{X}$,

$$|\eta(x) - \eta(x')| \leq L\|x - x'\|. \quad (4.1)$$

In order to stay exposition friendly, we will stay close to the Lipschitz condition by imposing the mildest assumptions, as found in [18]. We assume that we are given the *raw* data in $\mathcal{X} \times \mathcal{Y}$, where $\mathcal{X} \subset \mathbb{R}^D$. Our reference point will be Theorem 6.2 from [18] which states that if \mathcal{X} is bounded and $\eta(x)$ is L -Lipschitz, then

$$\mathbb{E}_n[(R_X)_{n,k}] - R_X^* = \mathcal{O}\left(\frac{1}{\sqrt{k}}\right) + \mathcal{O}\left(L\left(\frac{k}{n}\right)^{1/D}\right). \quad (4.2)$$

The main result of this section is an extension of the above to *transformed* data.

Theorem 4.1. *Let $\mathcal{X} \subseteq \mathbb{R}^D$ and $\tilde{\mathcal{X}} \subseteq \mathbb{R}^d$ be bounded sets, and let (X, Y) be a random vector taking values in $\mathcal{X} \times \{0, 1\}$. Let $g: \tilde{\mathcal{X}} \rightarrow \mathbb{R}$ be an L_g -Lipschitz function. Then for all transformations $f: \mathcal{X} \rightarrow \tilde{\mathcal{X}}$, one has*

$$\mathbb{E}_n[(R_{f(X)})_{n,k}] - R_X^* = \mathcal{O}\left(\frac{1}{\sqrt{k}}\right) + \mathcal{O}\left(L_g\left(\frac{k}{n}\right)^{1/d}\right) + \mathcal{O}\left(\sqrt[4]{\mathcal{L}_{g,X}(f)}\right). \quad (4.3)$$

Implications. An obvious comparison of (4.2) and (4.3) shows that applying a transformation can introduce a non-negligible bias, and thus a feature transformation should not be used if one has an infinite pool of data points. However, as we will confirm in the experimental section, in the finite-sample regime the benefit of reducing the dimension and, often more importantly, changing the geometry of the space using (pre-trained) transformations significantly outweighs the loss introduced through this bias. In practice, g is typically chosen to be a linear layer with the sigmoid output function, that is $g_w(x) = \sigma(\langle w, x \rangle)$, where $\sigma(x) := (1 + e^{-x})^{-1}$. It is easy to see that σ is $1/4$ -Lipschitz since $d\sigma/dx = \sigma(1 - \sigma) \leq 1/4$, whereas $x \mapsto \langle w, x \rangle$ is $\|w\|_2$ -Lipschitz by the Cauchy-Schwarz inequality, implying that g_w is $\|w\|_2/4$ -Lipschitz. Therefore, for any w we can simply insert $\mathcal{L}_{g_w,X}$ and $\|w\|_2$, since they comprise a valid bound in (4.3). In particular, this aligns with a common heuristic of minimizing a loss, while introducing the additional task of capturing $\|w\|_2$ in the process.

The proof of Theorem 4.1 is divided into two parts, motivated by

$$\mathbb{E}_n[(R_{f(X)})_{n,k}] - R_X^* = \underbrace{\mathbb{E}_n[(R_{f(X)})_{n,k}] - R_{f(X)}^*}_{\text{convergence rates of vanilla kNN on } f(X)} + \underbrace{R_{f(X)}^* - R_X^*}_{\text{safety of } f}. \quad (4.4)$$

We examine these parts in the next two sections.

4.1 Safe Transformations

We start by bounding the increase in the Bayes error that a transformation can introduce. In order to motivate what follows, note that one can rewrite $\Delta_{f,X}^*$ as²

$$\Delta_{f,X}^* = \mathbb{E}_{x \sim X} [p(y_x | x) - p_{f^{-1}}(y_{f(x)} | f(x))], \quad (4.5)$$

where $y_x = \arg \max_{y \in \mathcal{Y}} p(y|x)$ and $y_{f(x)} = \arg \max_{y \in \mathcal{Y}} p_{f^{-1}}(y|f(x))$. It is clear that any feature transformation can only increase the Bayes error (as seen in Figure 2a), due to the fact that $\max(\cdot)$ is a convex function. Hence, in order to understand and control this increase, we define and analyze *safe* transformations – those which increase the Bayes error only for a small value.

²When a deterministic feature transformation $f: \mathcal{X} \rightarrow \tilde{\mathcal{X}}$ is applied, we define the induced joint probability by $p_{f^{-1}}(\tilde{x}, y) = p(X \in f^{-1}(\{\tilde{x}\}), Y = y)$, where $f^{-1}(\{\tilde{x}\}) = \{x \in \mathcal{X}: f(x) = \tilde{x}\}$ is the preimage of \tilde{x} .

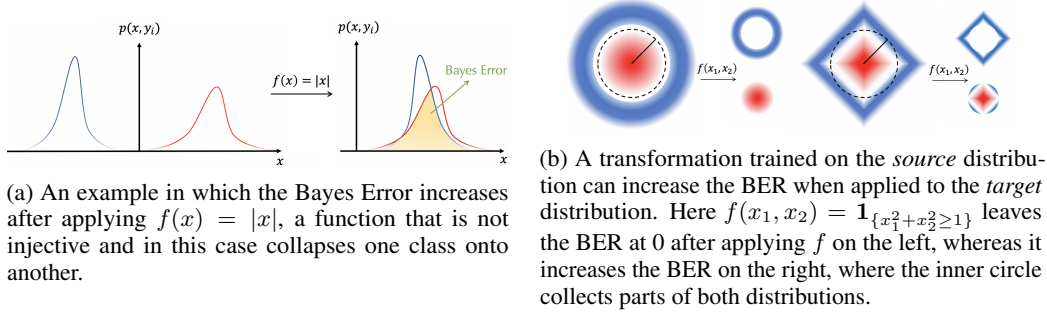


Figure 2: Transformations introduce bias by increasing the BER.

Definition 4.2. We say that a transformation $f: \mathcal{X} \rightarrow \tilde{\mathcal{X}}$ is δ -safe (with respect to p) if $\Delta_{f,X}^* \leq \delta$, and δ -unsafe (with respect to p) if there is no $\delta' < \delta$ such that $\Delta_{f,X}^* \leq \delta'$. When $\delta = 0$ we simply say that a function is safe or unsafe.

Motivated by (4.5), we see that any injective function f is safe, since for all $x \in \mathcal{X}$ one has $f^{-1}(\{f(x)\}) = \{x\}$. For example, this implies that $x \mapsto (x, f(x))$ is a safe transformation, for any map f . In the supplementary material we weaken the notion of injectivity, allowing us to deduce that the CReLU (Concatenated ReLU) activation function [31], defined as $x \mapsto (x^+, x^-)$, where $x^+ = \max\{x, 0\}$ and $x^- = \max\{-x, 0\}$, is a safe function. Interestingly, both x^+ and x^- are 1/2-unsafe, showing that unsafe functions can be concatenated into a safe one.

When discussing safety using injective functions, one is restricted to only considering how f behaves on \mathcal{X} , without using the information that \mathcal{Y} might facilitate. For example, a function that reduces the dimension is not injective, whilst in reality we might be able to avoid the loss of information that \mathcal{Y} carries about \mathcal{X} , when it comes to the Bayes error. A perfect such example is the map $f_{\mathcal{Y}}: \mathcal{X} \rightarrow \mathcal{Y}$ defined by $f_{\mathcal{Y}}(x) := y_x$, as $y_{f_{\mathcal{Y}}(x)} = \arg \max_{y \in \mathcal{Y}} p_{f_{\mathcal{Y}}^{-1}}(y|f_{\mathcal{Y}}(x)) = \arg \max_{y \in \mathcal{Y}} p_{f_{\mathcal{Y}}^{-1}}(y|y_x) = y_x$. Through (4.5) we see that $f_{\mathcal{Y}}$ does not change the Bayes error even though it reduces the size (of $\tilde{\mathcal{X}}$) to the number of classes. Thus, we now provide an alternative sufficient condition for δ -safe functions, which takes into account both \mathcal{X} and \mathcal{Y} through the *Kullback-Leibler divergence*³, given by

$$D_{KL}(q_1(x) \parallel q_2(x)) := \sum_{x \in \mathcal{X}} q_1(x) \log \frac{q_1(x)}{q_2(x)}.$$

We further denote $D_{KL}(p(y|x) \parallel p_{f^{-1}}(y|f(x))) := D_{KL}\left(p(x, y) \parallel \frac{p(x)}{p_{f^{-1}}(f(x))} p_{f^{-1}}(f(x), y)\right)$, which one can think of as the loss in the *mutual information* after applying f .

Lemma 4.3. Let \mathcal{X} and \mathcal{Y} be finite sets, and let $f: \mathcal{X} \rightarrow \tilde{\mathcal{X}}$ be a transformation such that $D_{KL}(p(y|x) \parallel p_{f^{-1}}(y|f(x))) \leq (2/\ln 2)\delta^2$. Then f is δ -safe.

We remark that the converse of Lemma 4.3 does not hold, meaning that one can have a δ -safe function for which the corresponding KL divergence is larger than $(2/\ln 2)\delta^2$. For example, the above mentioned $f_{\mathcal{Y}}$ is a safe transformation, whereas the KL-divergence is strictly positive as soon as $p(y|x) \neq p_{f^{-1}}(y|f(x))$, for some x and y , which is easy to construct. On the other hand, we can prove that the bounds are tight in the following sense.

Lemma 4.4. Let $\mathcal{X}, \tilde{\mathcal{X}}$ be finite sets satisfying $|\tilde{\mathcal{X}}| < |\mathcal{X}|$, $\mathcal{Y} = \{0, 1\}$, and let $f: \mathcal{X} \rightarrow \tilde{\mathcal{X}}$ be a transformation. For any $\delta \in [0, 1/2)$ there exist random variables X, Y , taking values in \mathcal{X}, \mathcal{Y} , such that $R_{f(X)}^* - R_X^* = \delta$ and $D_{KL}(p(y|x) \parallel p_{f^{-1}}(y|f(x))) = (2/\ln 2)\delta^2 + O(\delta^4)$.

A key challenge with the proposed approach is that the feature transformation might have been trained on a significantly different joint probability distribution, and, as such, might change the Bayes error in an unfavourable way when applied to our distribution of interest (Figure 2b). It is clear that in the worst case this can induce an unbounded error in the estimation. In practice, however, these feature transformations are learned for each domain specifically (e.g. deep convolutional neural networks for the vision domain, transformers for NLP tasks), and recent results in transfer learning show that such transformations do indeed *transfer* to a variety of downstream tasks [43]. Guided by this intuition we derive a sufficient condition under which our notion of safety is preserved on similar distributions.

³Without loss of generality, we assume that \mathcal{X} is finite and logarithm to the base 2.

Theorem 4.5. Let p_S and p_T be two probability distributions defined on $\mathcal{X} \times \mathcal{Y}$ that satisfy $D_{KL}(p_S || p_T) \leq \varepsilon^2/(8 \ln 2)$. If a transformation f is δ -safe with respect to p_S , then f is $(\delta + \varepsilon)$ -safe with respect to p_T .

From (4.2) we know that a kNN classifier on $f(X)$ converges to $R_{f(X)}^*$ under some mild assumptions. Since one aims at solving the original task, in other words to examine the convergence of $(R_{f(X)})_{n,k}$ to R_X^* , we need to make the transition to R_X^* by using some form of $\mathcal{L}_{g,X}(f)$. We conclude this section by stating the theorem that allows this transition.

Theorem 4.6. For every transformation $f: \mathcal{X} \rightarrow \tilde{\mathcal{X}}$, one has $\Delta_{f,X}^* \leq 2\sqrt{\mathcal{L}_{g,X}(f)}$.

4.2 Convergence Rates of a kNN Classifier over Transformed Features

In this section we derive convergence rates over transformed features, which together with Theorem 4.6 yield the proof of Theorem 4.1, via (4.4). We provide statements for X , i.e. the raw data, keeping in mind that we apply the main theorem of this section on $f(X)$ later on. In order to get a convergence rate that works on $f(X)$ without imposing any particular structure on f , one needs a weaker notion than the Lipschitz condition. It suffices to define the *probabilistic Lipschitz condition*.

Definition 4.7. Let $\varepsilon, \delta, L > 0$, and let $X, X' \in \mathcal{X}$ be random variables sampled using the same joint probability distribution p on $\mathcal{X} \times \{0, 1\}$. We say that $\eta(x) = p(1|x)$ is (ε, δ, L) -probably Lipschitz if

$$\mathbb{P}\left(|\eta(X) - \eta(X')| \leq \varepsilon + L\|X - X'\|\right) \geq 1 - \delta.$$

With such a condition, similar to the one of Theorem 6.2 in [18], we can prove the following result.

Theorem 4.8. Let $\mathcal{X} \subseteq \mathbb{R}^d$ be a bounded set, $X \in \mathcal{X}$, $Y \in \{0, 1\}$. If $\eta(x)$ is (ε, δ, L) -probably Lipschitz, then

$$\mathbb{E}_n[(R_X)_{n,k}] - R_X^* = \mathcal{O}\left(\frac{1}{\sqrt{k}}\right) + \mathcal{O}\left(L\left(\frac{k}{n}\right)^{1/d}\right) + \mathcal{O}(\sqrt{\delta} + \varepsilon). \quad (4.6)$$

The first term represents the variance in the training set, the second term comes from the Lipschitz-like structure of X , whilst the last term comes from the need of the probabilistic Lipschitz condition, which will later allow us to avoid additional constraints on f . We use Theorem 4.8 on $f(X)$, which needs an evidence of probably Lipschitz condition with respect to the g -squared loss. The following consequence of Markov's inequality yields the desired evidence. Since it is applied on $f(X)$, it suffices to have the identity function in place of f .

Lemma 4.9. Let g be an L -Lipschitz function. Then for any real number $\varepsilon > 0$, the function $\eta(x)$ is $(\varepsilon, 8\mathcal{L}_{g,X}(id)/\varepsilon^2, L)$ -probably Lipschitz.

Proof sketch of the main result. Deducing Theorem 4.1 is now straightforward – Lemma 4.9 says that we can apply Theorem 4.8 with X substituted by $f(X)$, meaning that for any f and any $\varepsilon > 0$,

$$\mathbb{E}_n[(R_{f(X)})_{n,k}] - R_{f(X)}^* = \mathcal{O}\left(\frac{1}{\sqrt{k}}\right) + \mathcal{O}\left(L\left(\frac{k}{n}\right)^{1/d}\right) + \mathcal{O}\left(\frac{\sqrt{\mathcal{L}_{g,f(X)}(id)}}{\varepsilon} + \varepsilon\right). \quad (4.7)$$

We optimize this by setting $\varepsilon = \sqrt[4]{\mathcal{L}_{g,f(X)}(id)}$. In the supplementary material, we prove an easily attainable upper bound $\mathcal{L}_{g,f(X)}(id) \leq \mathcal{L}_{g,X}(f)$, which, together with the final transition from $R_{f(X)}^*$ to R_X^* that is available via Theorem 4.6, proves the main result.

Discussions. We could further optimize the exponent of $\mathcal{L}_{g,X}$, however, we leave this for future work, as it already serves our purpose of providing a connection between the g -squared loss of f and the Lipschitz constant of g . Furthermore, one might argue that (4.2) could be used to yield a better rate of convergence than the one in (4.3), provided that the Lipschitz constant of $\eta_{f^{-1}}$ is known for every f . However, checking whether $\eta_{f^{-1}}$ is L -Lipschitz is not a feasible task. For example, computing the best Lipschitz constant of a deep neural network is an NP-hard problem [29], whilst upper bounding the Lipschitz constant over high-dimensional real-world data and many transformations becomes impractical. Our result provides a practical framework that can easily be deployed for studying the influence of feature transformations on a kNN classifier, as illustrated in the next section.

Table 1: Dataset Statistics

NAME	DIMENSION	CLASSES	TRAINING SAMPLES	TEST SAMPLES
MNIST	784	10	60K	10K
CIFAR10	3072	10	50K	10K
CIFAR100	3072	100	50K	10K
IMDB	104083	2	25K	25K
SST2	14583	2	67K	872
YELP	175710	5	500K	50K

5 Experimental Results

The goal of this section is to show that one can use the upper bounds on the convergence rate of kNN, derived in the previous sections, to explain the impact of different feature transformations on the kNN performance. This works particularly well when compared with simpler metrics mentioned in the introduction, such as the dimension or the accuracy of another trained classifier on the same space.

In order to empirically verify our theoretical results, as discussed in the implications of Theorem 4.1, we focus on the logistic regression model, since it is most commonly used in practice, and for which one can easily calculate the Lipschitz constant. More precisely, we examine $g(x) = \sigma(\langle w, x \rangle)$, with $L_g = \|w\|_2$. When dealing with multi-class tasks, we use

$$g(x) = \text{softmax}(W^T x + b),$$

whilst reporting $\|W\|_F$, the Frobenius norm of the weights, in place of $\|w\|_2$.

Calculating the g -squared loss of f is not feasible in practice, since one usually does not know the true distribution $\eta(X)$. However, using the fact that $\mathbb{E}_{Y|X=x}(\eta(x) - Y) = 0$, one can decompose the loss as

$$\mathcal{L}_{g,X}(f) = \mathbb{E}_{X,Y}((g \circ f)(X) - Y)^2 + \mathbb{E}_{X,Y}(\eta(X) - Y)^2.$$

As the second term does not depend on g or f , we can rank feature transformations by estimating the first term for a fixed g . With that in mind, when we compare different transformations, we report the *mean squared error*⁴ of the test set, defined by

$$MSE_g(f, W, b) = \frac{1}{|TEST|} \sum_{i \in TEST} (\text{softmax}(W^T f(x_i) + b) - y_i)^2.$$

For kNN, we restrict ourselves to the Euclidean distance, the most commonly used distance function. Furthermore, we set $k = 1$ for this entire section, whereas the empirical analysis of the influence of $k > 1$ is conducted in Section B of the supplementary material.

5.1 Datasets

We perform the evaluation on two data modalities which are ubiquitous in modern machine learning. The first group consists of *visual classification tasks*, including MNIST, CIFAR10 and CIFAR100. The second group consists of standard *text classification tasks*, where we focus on IMDB, SST2 and YELP. The details are presented in Table 1. We remark that for the visual classification tasks, the raw features are the pixel intensities, whereas for the text classification we apply the standard bag-of-words preprocessing, with and without term-frequency/inverse-document-frequency weighting [22].

5.2 Feature Transformations

We run the experiments on a diverse set of feature transformations used in practice. The list of 30 transformations includes standard dimension reduction methods like the Principal Component Analysis (PCA) and Neighborhood Component Analysis (NCA), as well as using pre-trained feature extraction networks available in TensorFlow Hub and PyTorch Hub. A complete list of the used transformations per dataset is given in the supplementary material.

⁴In these terms, when one wants to rank different classifiers, the MSE is often referred to as the *Brier score* (we refer an interested reader to [6, 8]).

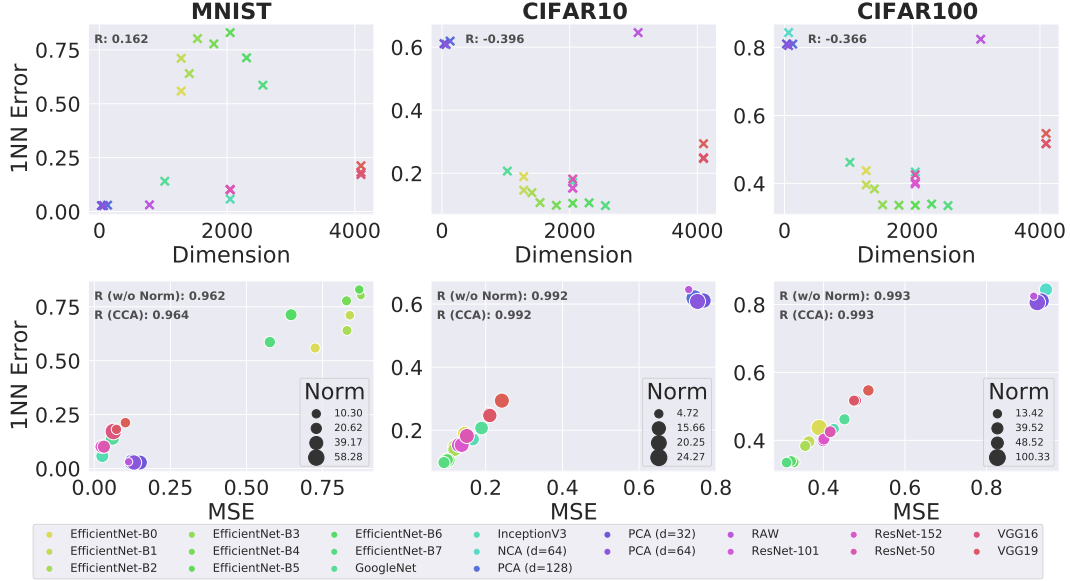


Figure 3: Results on computer vision datasets. **(Top row)** There is a poor linear correlation between the feature dimension and the 1NN error. **(Bottom row)** Comparing the 1NN error with the MSE shows a very high linear correlation. Combining MSE with the norm marginally improves the correlation coefficients.

5.3 Results

We use *Pearson’s r correlation* [5] to analyze different approaches for comparing feature transformations with respect to the kNN error. Pearson’s r ranges from -1 to 1, with 1 implying that two random variables have a perfect positive (linear) correlation, where -1 implies a perfect negative correlation. We provide an extended experimental evaluation including convergence plots and a detailed description of the experimental setting (such as the protocol used for training W) in Section B of the supplementary material.

Feature Dimension. We start by inspecting the dimension of the resulting feature space and its achieved kNN error. We exhibit a very poor (or even negative) correlation on all text datasets, as illustrated in the top rows of Figures 3 and 4.

MSE vs 1NN Error. On computer vision tasks we observe high correlation when comparing the 1NN error with the MSE, with marginal improvements when the norm is included, as reported in the bottom row of Figure 3. This is in line with (4.3) by simply concluding that the last term dominates.

On text classification datasets the MSE alone struggles to explain the performance of 1NN on top of feature transformations, as visible in the bottom row of Figure 4. Without considering the norm (i.e., ignoring the size of the circles on Figure 4), we see a number of misjudged (important) examples, despite having a positive correlation.

Validation Based on Our Theoretical Results – MSE and Norm. In order to report the correlation between multiple variables (notably the 1NN error vs. the combination of MSE and the norm), we first reduce the dimension of the latter by performing a canonical-correlation analysis (CCA) [35] which enables us to evaluate Pearson’s r afterwards.

As visible in the second row of Figure 4, there is a significant improvement in correlation on all the text classification datasets. Furthermore, this method enables us to separate transformations that achieve similar MSE, but with different norms, in particular on those transformations that perform well. We can see that in those cases, the smaller norm implies smaller 1NN error. Including the norm into the analysis of computer vision datasets, we see some marginal improvements, although on already high correlation values, which is also aligned with our theoretical analysis.

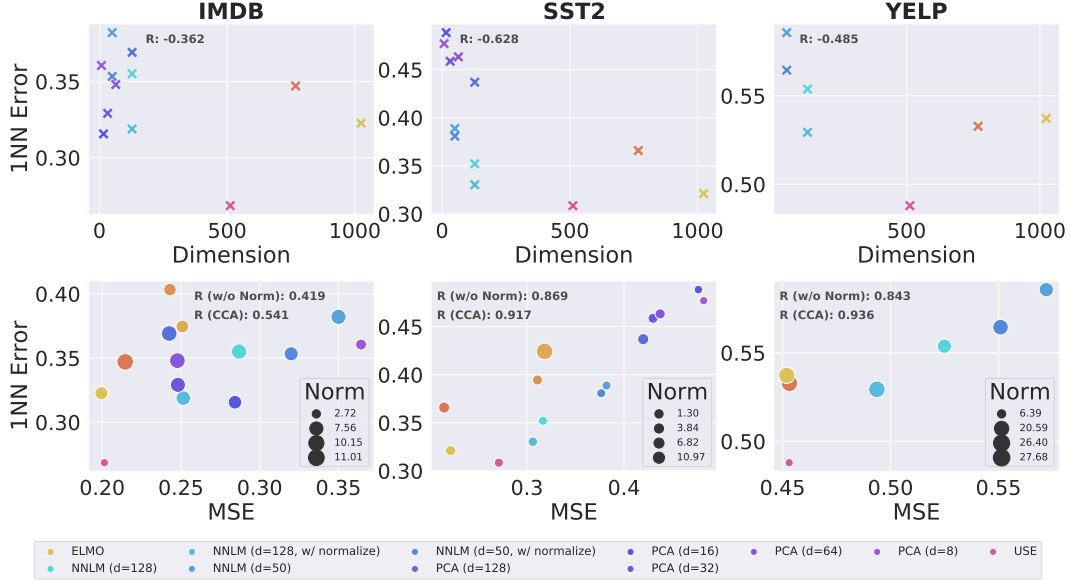


Figure 4: Results on text classification datasets. **(Top row)** There is a poor linear correlation between the feature dimension and the 1NN error. **(Bottom row)** Comparing the 1NN error with MSE without the norm (i.e., by ignoring the sizes of the circles) leads a strong positive correlation. Including the norm improves this further, particularly on important cases (the bottom left corner) which makes the inclusion of norm significant.

Empirical Results for $k > 1$. In addition to the experiments presented in the previous section, we performed experiments for $k > 1$ over all datasets and all embeddings. All the results for $k > 1$ confirm the theoretical findings, whilst for some k they offer an improvement in the linear correlation (e.g., on SST2 one can get CCA score up to 0.97 when $k = 8$, whereas in Figure 4 we report 0.917, for $k = 1$). In order to simplify the exposition, we opted for $k = 1$ and MSE instead of $MSE^{1/4}$ since it already serves the purpose of showing that MSE is important on its own, whereas including the smoothness assumption through the norm further improves the correlation.

6 Final remarks

One could examine the tightness of our theoretical bounds by constructing a toy dataset with a known true posterior probability and a set of transformations. However, any such transformation should either be an identity (if the toy dataset already has the desired property), or carefully constructed for this purpose only. In this work we opted for not constructing a single transformation ourselves, as our main goal is to bridge the gap between the real-world applications (e.g. pre-trained embeddings) with the theory of nearest neighbors. For example, even Lemma 4.4, which establishes the sharpness of the safety bound, works for any transformation. For that purpose, our probabilistic Lipschitz condition is as weak as possible. To this end, studying CCA of $k^{-1/2}$, $\|w\|(k/n)^{1/d}$ and $MSE^{1/4}$ (or some other exponent under stronger assumptions) for $k > 1$, could provide another angle for understanding the tightness of the bound, which is out of the scope of this work.

Conclusion. The goal of this work is to provide novel theoretical results aimed towards understanding the convergence behavior of kNN classifiers over transformations, bridging the existing gap between the current state of the theory and kNN applications used in practice. We provide a rigorous analysis of properties of transformations that are highly correlated with the performance of kNN classifiers, yielding explainable results of kNN classifiers over transformations. We believe that optimizing the upper bound presented here and extending results to classifiers other than logistic regression could form an interesting line of future research.

Acknowledgements

We are grateful to Mario and André for their constructive feedback. CZ and the DS3Lab gratefully acknowledge the support from the Swiss National Science Foundation (Project Number 200021_184628), Innosuisse/SNF BRIDGE Discovery (Project Number 40B2-0_187132), European Union Horizon 2020 Research and Innovation Programme (DAPHNE, 957407), Botnar Research Centre for Child Health, Swiss Data Science Center, Alibaba, Cisco, eBay, Google Focused Research Awards, Oracle Labs, Swisscom, Zurich Insurance, Chinese Scholarship Council, and the Department of Computer Science at ETH Zurich.

Broader Impact

One of the current bottlenecks in machine learning is the lack of robustness and explainability. It is well known that kNN has properties (some of them cited in the introduction) that allow one to tackle these challenges. However, when it comes to accuracy, kNN on its own is often inferior to modern day machine learning methods, limiting the possible impact. In this paper we propose a novel theoretical framework aimed at understanding the best practices for employing kNN on top of pre-trained feature transformations, in order to gain on all positive aspects of kNN. In particular, we show that by using resources that are already widely available (i.e., open-sourced pre-trained embeddings), without the need of training from scratch, one can improve this already efficient, robust and interpretable classifier. We do not expect any direct negative impact from this work as we purely focus on the theoretical understanding of a classifier that itself is non-controversial.

References

- [1] Naomi S. Altman. “An introduction to kernel and nearest-neighbor nonparametric regression”. In: *The American Statistician* 46.3 (1992), pp. 175–185.
- [2] András Antos, Luc Devroye, and László Györfi. “Lower bounds for Bayes error estimation”. In: *IEEE Transactions on Pattern Analysis and Machine Intelligence* 21.7 (1999), pp. 643–645.
- [3] Jean-Yves Audibert and Alexandre B. Tsybakov. “Fast learning rates for plug-in classifiers”. In: *Annals of Statistics* 35.2 (2007), pp. 608–633.
- [4] Dara Bahri, Heinrich Jiang, and Maya Gupta. “Deep k-NN for Noisy Labels”. In: *arXiv preprint arXiv:2004.12289* (2020).
- [5] Jacob Benesty et al. “Pearson correlation coefficient”. In: *Noise reduction in speech processing*. Springer, 2009, pp. 1–4.
- [6] Glenn W. Brier. “Verification of forecasts expressed in terms of probability”. In: *Monthly weather review* 78.1 (1950), pp. 1–3.
- [7] Kamalika Chaudhuri and Sanjoy Dasgupta. “Rates of convergence for nearest neighbor classification”. In: *Advances in Neural Information Processing Systems*. 2014, pp. 3437–3445.
- [8] Ira Cohen and Moises Goldszmidt. “Properties and benefits of calibrated classifiers”. In: *European Conference on Principles of Data Mining and Knowledge Discovery*. Springer, 2004, pp. 125–136.
- [9] Thomas M. Cover. “Rates of convergence for nearest neighbor procedures”. In: *Proceedings of the Hawaii International Conference on Systems Sciences*. 1968, pp. 413–415.
- [10] Thomas M. Cover and Peter A. Hart. “Nearest neighbor pattern classification”. In: *IEEE Transactions on Information Theory* 13.1 (1967), pp. 21–27.
- [11] Thomas M. Cover and Joy A. Thomas. *Elements of Information Theory 2nd Edition* (Wiley Series in Telecommunications and Signal Processing). Wiley-Interscience, 2006.
- [12] Pierre A. Devijver. “A multiclass, k-NN approach to Bayes risk estimation”. In: *Pattern recognition letters* 3.1 (1985), pp. 1–6.
- [13] Maik Döring, László Györfi, and Harro Walk. “Rate of convergence of k-nearest-neighbor classification rule”. In: *The Journal of Machine Learning Research* 18.1 (2017), pp. 8485–8500.
- [14] Jozsef Fritz. “Distribution-free exponential error bound for nearest neighbor pattern classification”. In: *IEEE Transactions on Information Theory* 21.5 (1975), pp. 552–557.
- [15] Sébastien Gadat, Thierry Klein, and Clément Marteau. “Classification in general finite dimensional spaces with the k-nearest neighbor rule”. In: *The Annals of Statistics* 44.3 (2016), pp. 982–1009.

- [16] Jacob Goldberger et al. “Neighbourhood components analysis”. In: *Advances in Neural Information Processing Systems*. 2005, pp. 513–520.
- [17] L Györfi. “The Rate of Convergence of kn-NN Regression Estimates and Classification Rule”. In: *IEEE Transactions on Information Theory* 27.3 (1981), pp. 357–362.
- [18] László Györfi et al. *A distribution-free theory of nonparametric regression*. Springer Series in Statistics. Springer-Verlag, New York, 2002, pp. xvi+647.
- [19] Ruoxi Jia et al. “An Empirical and Comparative Analysis of Data Valuation with Scalable Algorithms”. In: *arXiv preprint arXiv:1911.07128* (2019).
- [20] Ruoxi Jia et al. “Efficient task-specific data valuation for nearest neighbor algorithms”. In: *Proceedings of the VLDB Endowment* 12.11 (2019), pp. 1610–1623.
- [21] Ruoxi Jia et al. “Towards Efficient Data Valuation Based on the Shapley Value”. In: *The 22nd International Conference on Artificial Intelligence and Statistics*. 2019, pp. 1167–1176.
- [22] Karen Sparck Jones. “A statistical interpretation of term specificity and its application in retrieval”. In: *Journal of Documentation* (1972).
- [23] Juraj Kacur, Radoslav Vargic, and Pavol Mulinka. “Speaker identification by K-nearest neighbors: Application of PCA and LDA prior to KNN”. In: *2011 18th International Conference on Systems, Signals and Image Processing*. IEEE. 2011, pp. 1–4.
- [24] Bojan Karlaš et al. “Nearest Neighbor Classifiers over Incomplete Information: From Certain Answers to Certain Predictions”. In: *arXiv preprint arXiv:2005.05117* (2020).
- [25] Michael Kohler and Adam Krzyżak. “On the rate of convergence of local averaging plug-in classification rules under a margin condition”. In: *IEEE Transactions on Information Theory* 53.5 (2007), pp. 1735–1742.
- [26] Sanjeev R Kulkarni and Steven E Posner. “Rates of convergence of nearest neighbor estimation under arbitrary sampling”. In: *IEEE Transactions on Information Theory* 41.4 (1995), pp. 1028–1039.
- [27] Nazila Panahi et al. “Recognition of different datasets using PCA, LDA, and various classifiers”. In: *2011 5th International Conference on Application of Information and Communication Technologies (AICT)*. IEEE. 2011, pp. 1–5.
- [28] Nicolas Papernot and Patrick McDaniel. “Deep k-nearest neighbors: Towards confident, interpretable and robust deep learning”. In: *arXiv preprint arXiv:1803.04765* (2018).
- [29] Kevin Scaman and Aladin Virmaux. “Lipschitz regularity of deep neural networks: analysis and efficient estimation”. In: *Advances in Neural Information Processing Systems* 31. 2018, pp. 3835–3844.
- [30] Glenn Shafer and Vladimir Vovk. “A tutorial on conformal prediction”. In: *Journal of Machine Learning Research* 9 (2008), pp. 371–421.
- [31] Wenling Shang et al. “Understanding and Improving Convolutional Neural Networks via Concatenated Rectified Linear Units”. In: *Proceedings of the 33rd International Conference on International Conference on Machine Learning*. Vol. 48. 2016, pp. 2217–2225.
- [32] Robert R Snapp, Demetri Psaltis, and Santosh S Venkatesh. “Asymptotic slowing down of the nearest-neighbor classifier”. In: *Advances in Neural Information Processing Systems*. 1991, pp. 932–938.
- [33] Robert R Snapp and Tong Xu. “Estimating the bayes risk from sample data”. In: *Advances in Neural Information Processing Systems*. 1996, pp. 232–238.
- [34] Charles J Stone. “Consistent nonparametric regression”. In: *The Annals of Statistics* (1977), pp. 595–620.
- [35] Bruce Thompson. “Canonical correlation analysis”. In: *Encyclopedia of statistics in behavioral science* (2005).
- [36] Bruno Trstenjak, Sasa Mikac, and Dzenana Donko. “KNN with TF-IDF based framework for text categorization”. In: *Procedia Engineering* 69 (2014), pp. 1356–1364.
- [37] Alexander B Tsybakov. “Optimal aggregation of classifiers in statistical learning”. In: *The Annals of Statistics* 32.1 (2004), pp. 135–166.
- [38] Terry J. Wagner. “Convergence of the nearest neighbor rule”. In: *IEEE Transactions on Information Theory* 17.5 (1971), pp. 566–571.
- [39] Yizhen Wang, Somesh Jha, and Kamalika Chaudhuri. “Analyzing the Robustness of Nearest Neighbors to Adversarial Examples”. In: *Proceedings of the 35th International Conference on Machine Learning*. Vol. 80. 2018, pp. 5133–5142.

- [40] Zhiguo Wang, Wael Hamza, and Linfeng Song. “ k -Nearest Neighbor Augmented Neural Networks for Text Classification”. In: *arXiv preprint arXiv:1708.07863* (2017).
- [41] Maurice Weber et al. “RAB: Provable Robustness Against Backdoor Attacks”. In: *arXiv preprint arXiv:2003.08904* (2020).
- [42] Zhirong Wu, Alexei A Efros, and Stella X Yu. “Improving generalization via scalable neighborhood component analysis”. In: *Proceedings of the European Conference on Computer Vision (ECCV)*. 2018, pp. 685–701.
- [43] Xiaohua Zhai et al. “The visual task adaptation benchmark”. In: *arXiv preprint arXiv:1910.04867* (2019).

A Proofs

A.1 Safe Transformations

In this section we prove the claims from Section 4.1, in the same order as stated there. Even though the main part of the paper is considering $\mathcal{Y} = \{0, 1\}$ only, which is the usual setting when convergence rates of a kNN classifier are discussed, we suppose that $\mathcal{Y} = \{1, \dots, C\}$, for some integer $C \geq 2$, until Section A.1.1.

Safe Transformations via Injectivity

We discuss injective functions in Section 4.1, and provide examples of safe transformations that arise from injectivity, such as $x \mapsto (x, f(x))$, for any map f , and $x \mapsto (x^+, x^-)$. We will now prove this by providing a sufficient condition for a function to be δ -safe. We call this condition δ -injectivity.

Definition A.1. Let $(\mathcal{X}, \mathcal{A}, p)$ and be a finite probability space, and let $(\tilde{\mathcal{X}}, \tilde{\mathcal{A}})$ be a finite measurable space. We say that a measurable function $f: \mathcal{X} \rightarrow \tilde{\mathcal{X}}$ is δ -injective if there exists a subset $I_{\mathcal{X}}(f) \subseteq \mathcal{X}$ on which f is injective, and that satisfies

$$p(I_{\mathcal{X}}(f)) \geq 1 - \delta.$$

Lemma A.2. Let $f_i: \mathcal{X} \rightarrow \tilde{\mathcal{X}}_i$, for $i = 0, \dots, n$, be functions such that there exist $I_{\mathcal{X}}(f_0), \dots, I_{\mathcal{X}}(f_n) \subseteq \mathcal{X}$, sets on which f_0, \dots, f_n are injective, respectively, and such that

$$p\left(\bigcup_{i=0}^n I_{\mathcal{X}}(f_i)\right) \geq (1 - \delta).$$

Then $(f_0, \dots, f_n): \mathcal{X} \rightarrow \prod_{i=0}^n \tilde{\mathcal{X}}_i$ is δ -safe.

In particular, if f_0 is δ -injective, then (f_0, f_1, \dots, f_n) is δ -safe.

PROOF: We first prove the claim for $n = 0$ and then extend it to $n \in \mathbb{N}$.

(1) $n = 0$:

In this case, we ought to prove that if f is δ -injective, then f is δ -safe. Let $I_{\mathcal{X}}(f)$ be a set on which f is injective and that satisfies $p(I_{\mathcal{X}}(f)) \geq 1 - \delta$. Motivated by (4.5), we define $\mathcal{X}_l := \{x \in \mathcal{X} : y_x \neq y_{f(x)}\}$. With the above definition, note that (4.5) can be reduced to

$$\Delta_{f,X}^* = \mathbb{E}_{x \sim X} [(p(y_x|x) - p_{f^{-1}}(y_{f(x)}|f(x))) \cdot 1\{x \in \mathcal{X}_l\}] \leq p(\mathcal{X}_l). \quad (\text{A.1})$$

We will now modify $I_{\mathcal{X}}(f)$ to get $I_{\mathcal{X}_l}$ that is of the same mass, and is disjoint from \mathcal{X}_l . If $\mathcal{X}_l \cap I_{\mathcal{X}}(f) = \emptyset$, then we are done. Therefore, let $x_l \in \mathcal{X}_l \cap I_{\mathcal{X}}(f)$, implying $y_{x_l} \neq y_{f(x_l)}$. Note that there has to exist $x \in f^{-1}(\{f(x_l)\})$ such that $y_x = y_{f(x_l)} = y_{f(x)}$, as otherwise $y_{f(x)}$ would not be the winning y for $f(x)$. We place x into $I_{\mathcal{X}_l}$, noting that $x \notin \mathcal{X}_l$, and repeat this for every element in $\mathcal{X}_l \cap I_{\mathcal{X}}(f)$. Finally, we add to $I_{\mathcal{X}_l}$ all the elements that are in $I_{\mathcal{X}}(f) \setminus \mathcal{X}_l$. By the construction we see that $I_{\mathcal{X}_l}$ is a set on which f is injective, since we always choose only one representative from each $f^{-1}(\hat{x})$, and

$$p(I_{\mathcal{X}_l}) = p(\mathcal{X}_l \sqcup (I_{\mathcal{X}}(f) \setminus \mathcal{X}_l)) = p(I_{\mathcal{X}}(f)) \geq 1 - \delta,$$

where \sqcup denotes a disjoint union. Since \mathcal{X}_l and $I_{\mathcal{X}_l}$ are disjoint, this yields $p(\mathcal{X}_l) < \delta$, which together with (A.1) finishes the proof.

(2) $n > 0$:

Let $I_{\mathcal{X}}(f_0, \dots, f_n) := \bigcup_{i=0}^n I_{\mathcal{X}}(f_i)$. It suffices to prove that (f_0, \dots, f_n) is injective on $I_{\mathcal{X}}(f_0, \dots, f_n)$, since we already have $p(I_{\mathcal{X}}(f_0, \dots, f_n)) \geq (1 - \delta)$.

Define $I'_{\mathcal{X}}(f_0), \dots, I'_{\mathcal{X}}(f_n)$ inductively by $I'_{\mathcal{X}}(f_0) := I_{\mathcal{X}}(f_0)$, and

$$I'_{\mathcal{X}}(f_k) := I_{\mathcal{X}}(f_k) \setminus \left(\bigcup_{j=0}^{k-1} I_{\mathcal{X}}(f_j) \right), \quad k = 1, \dots, n.$$

Then

$$I_{\mathcal{X}}(f_0, \dots, f_n) = \bigcup_{i=0}^n I_{\mathcal{X}}(f_i) = \bigsqcup_{i=0}^n I'_{\mathcal{X}}(f_i).$$

Therefore, it suffices to prove that (f_0, \dots, f_n) is injective on $\bigsqcup_{i=0}^n I'_{\mathcal{X}}(f_i)$.

Let $x, \tilde{x} \in \bigsqcup_{i=0}^n I'_{\mathcal{X}}(f_i)$, $x \neq \tilde{x}$, and let k, l be such that $x \in I'_{\mathcal{X}}(f_k)$, $\tilde{x} \in I'_{\mathcal{X}}(f_l)$. Then $f_{\max\{k,l\}}(x) \neq f_{\max\{k,l\}}(\tilde{x})$, for which we use that $I'_{\mathcal{X}}(f_{\max\{k,l\}})$ is injective, if $\tilde{x} \in I'_{\mathcal{X}}(f_{\max\{k,l\}})$, or that $I'_{\mathcal{X}}(f_{\max\{k,l\}})$ is disjoint from all the previous ones. This proves that $(f_0, \dots, f_n)(x) \neq (f_0, \dots, f_n)(\tilde{x})$, so (f_0, \dots, f_n) is injective on $\bigsqcup_{i=0}^n I'_{\mathcal{X}}(f_i)$.

To finish the proof, we note that if f_0 is δ -injective, then

$$p\left(\bigcup_{i=0}^n I_{\mathcal{X}}(f_i)\right) \geq p(I_{\mathcal{X}}(f_0)) \geq (1 - \delta),$$

implying that (f_0, \dots, f_n) is δ -safe, by the results in the previous paragraph. \square

Safe Transformations via Information Theory

In this section we prove Lemmas 4.3 and 4.4. The *mutual information* between random variables X and Y , taking values in finite sets \mathcal{X} and \mathcal{Y} , is defined as

$$I(X; Y) := D_{KL}(p(x, y) \parallel p(x)p(y)) = \sum_{x \in \mathcal{X}} \sum_{y \in \mathcal{Y}} p(x, y) \log \frac{p(x, y)}{p(x)p(y)},$$

where the logarithm is in base 2. Lemma 4.3 can be understood as the bound on the allowed loss in the mutual information, by noting that

$$\begin{aligned} I(X; Y) - I(f(X); Y) &= D_{KL}(p(x, y) \parallel p(x)p(y)) - D_{KL}(p_{f^{-1}}(f(x), y) \parallel p_{f^{-1}}(f(x))p_{f^{-1}}(y)) \\ &= \mathbb{E}_{p(x, y)} \log \frac{p(x, y)}{p(x)p(y)} - \mathbb{E}_{p(x, y)} \log \frac{p_{f^{-1}}(f(x), y)}{p_{f^{-1}}(f(x))p_{f^{-1}}(y)} \\ &= \mathbb{E}_{p(x, y)} \log \frac{p(y|x)}{p_{f^{-1}}(y|f(x))} = D_{KL}(p(y|x) \parallel p_{f^{-1}}(y|f(x))), \end{aligned} \quad (\text{A.2})$$

since $p_{f^{-1}}(y) = p(y)$. The proof of Lemma 4.3 starts by connecting the change in the Bayes error with the L^1 -norm of the distance between probability distributions, which, in a finite space, equals twice the *total variation distance*. We conclude the proof by applying *Pinsker's inequality*. For a detailed analysis of all of these terms we refer an interested reader to Chapter 11 in [11].

PROOF OF LEMMA 4.3: Note that (4.5) and the definitions of y_x and $y_{f(x)}$ yield

$$\begin{aligned} \Delta_{f, X}^* &= \mathbb{E}_{x \sim X} [p(y_x | x) - p_{f^{-1}}(y_{f(x)} | f(x))] \\ &= \mathbb{E}_{x \sim X} [p(y_x | x) - p_{f^{-1}}(y_x | f(x))] + \underbrace{\mathbb{E}_{x \sim X} [p_{f^{-1}}(y_x | f(x)) - p_{f^{-1}}(y_{f(x)} | f(x))]}_{\leq 0} \\ &\leq \frac{1}{2} |\mathbb{E}_{x \sim X} [p(y_x | x) - p_{f^{-1}}(y_x | f(x))]| + \frac{1}{2} \left| \mathbb{E}_{x \sim X} \sum_{y \neq y_x} [p(y | x) - p_{f^{-1}}(y | f(x))] \right| \\ &\leq \frac{1}{2} \mathbb{E}_{x \sim X} \sum_{y \in \mathcal{Y}} |p(y | x) - p_{f^{-1}}(y | f(x))| \\ &= \frac{1}{2} \left\| p(x, y) - \frac{p(x)}{p_{f^{-1}}(f(x))} p_{f^{-1}}(f(x), y) \right\|_1, \end{aligned}$$

where we introduced the sum by expanding

$$1 = p(y_x | x) + \sum_{y \neq y_x} p(y | x) = p_{f^{-1}}(y_x | f(x)) + \sum_{y \neq y_x} p_{f^{-1}}(y | f(x)),$$

whilst using the triangle inequality. Pinsker's inequality implies that

$$\left\| p(x, y) - \frac{p(x)}{p_{f^{-1}}(f(x))} p_{f^{-1}}(f(x), y) \right\|_1 \leq \sqrt{(2 \ln 2) D_{KL}(p(y | x) || p_{f^{-1}}(y | f(x)))} \leq 2\delta,$$

finishing the proof after dividing by 2. \square

Finally, we provide a construction which shows that the bound in Lemma 4.3 is of the right order.

PROOF OF LEMMA 4.4: Recall that we define $\eta(x) = p(1 | x)$. We start with $|\mathcal{X}| = 2$, since the general case will be a straightforward extension of it.

Let $\mathcal{X} = \{x_0, x_1\}$ and $\tilde{\mathcal{X}} = \{\tilde{x}\}$. We define p on $\mathcal{X} \times \mathcal{Y}$ by $p(x_0) = p(x_1) = 1/2$, and $\eta(x_0) = \frac{1}{2} - \delta$, $\eta(x_1) = \frac{1}{2} + \delta$, which defines $p(x, y)$. For the change in the Bayes error we have

$$\Delta_{f, X}^* = \frac{1}{2} - \sum_{x \in \{x_0, x_1\}} p(x) \min\{\eta(x), 1 - \eta(x)\} = \delta.$$

For the KL-divergence, note that

$$\begin{aligned} D_{KL}(p(y | x) || p_{f^{-1}}(y | f(x))) &= \sum_{x \in \{x_0, x_1\}} \sum_{y \in \{0, 1\}} p(x, y) \log \frac{p(y | x)}{p_{f^{-1}}(y | f(x))} \\ &= \sum_{x \in \{x_0, x_1\}} p(x) \sum_{y \in \{0, 1\}} p(y | x) \log 2p(y | x) \\ &= \sum_{x \in \{x_0, x_1\}} p(x) (\eta(x_0) \log 2\eta(x_0) + \eta(x_1) \log 2\eta(x_1)) \\ &= \frac{1}{2} ((1 - 2\delta) \log(1 - 2\delta) + (1 + 2\delta) \log(1 + 2\delta)), \end{aligned}$$

where we used $\eta(x_0) = \frac{1}{2} - \delta = 1 - \eta(x_1)$. Taylor expansion for $|x| < 1$ gives

$$(1 + x) \ln(1 + x) + (1 - x) \ln(1 - x) = 2 \sum_{k \in \mathbb{N}} \frac{1}{(2k - 1)2k} x^{2k},$$

which implies

$$\begin{aligned} D_{KL}(p(y | x) || p_{f^{-1}}(y | f(x))) &= \frac{1}{\ln 2} \sum_{k \in \mathbb{N}} \frac{2^{2k}}{(2k - 1)2k} \delta^{2k} \\ &= \frac{2}{\ln 2} \delta^2 + \frac{4}{3 \ln 2} \delta^4 + \frac{32}{15 \ln 2} \delta^6 + \dots = (2/\ln 2) \delta^2 + O(\delta^4), \end{aligned}$$

finishing the proof for $|\mathcal{X}| = 2$.

Suppose that $|\mathcal{X}| > 2$. Since $|\tilde{\mathcal{X}}| < |\mathcal{X}|$, we know that there exists a \tilde{x} such that $|f^{-1}(\tilde{x})| \geq 2$, so let $x_0, x_1 \in f^{-1}(\tilde{x})$ be distinct. We define p on $\mathcal{X} \times \mathcal{Y}$ as $p(x, y) = 0$ for $x \notin \{x_0, x_1\}$, while for $p(x_0, y), p(x_1, y)$ we do the above construction, which proves the lemma. \square

For $|\mathcal{X}| > 2$ we used the most simple construction, however, one can extend the idea behind the proof for $|\mathcal{X}| = 2$ into a more general one. For example, we can define a probability distribution in which for all $x \in \mathcal{X}$ one has $\eta(x) \in \{\frac{1}{2} - \delta, \frac{1}{2} + \delta\}$, with the same proportion of each. In other words, each x is a bucket with either $\frac{1}{2} - \delta$ values being 1, or $\frac{1}{2} + \delta$ values being 1. Let

$$\mathcal{X}_0 := \left\{ x \in \mathcal{X} : \eta(x) = \frac{1}{2} - \delta \right\}, \quad \mathcal{X}_1 := \left\{ x \in \mathcal{X} : \eta(x) = \frac{1}{2} + \delta \right\},$$

thus $\mathcal{X} = \mathcal{X}_0 \sqcup \mathcal{X}_1$. Now f can either merge buckets of the same type, in which case neither do the Bayes error nor the KL-divergence change, or buckets of a different type, where the changes are δ and $2\delta^2 + O(\delta^4)$, respectively. Choosing the right proportion of each bucket in $f^{-1}(\tilde{x})$ is now an easy task, yielding the construction.

Safe Transformations on Similar Probability Distributions

In this section we prove Theorem 4.5. As mentioned in the main body, transformations used for estimating the Bayes error might have been trained on a distribution different then the target one, and as such, might change the Bayes error in an unfavourable way when applied to the distribution of interest. We investigate this in the next few paragraphs.

Let $p_S(x, y)$ be the *source* probability distribution based on random variables $X_S \in \mathcal{X}_S$ and $Y_S \in \mathcal{Y}_S$, which is the probability distributions used for training a transformation f_S . With $p_T(x, y)$ we denote the *target* probability distribution, the one that serves as the basis for random variables $X_T \in \mathcal{X}_T$ and $Y_T \in \mathcal{Y}_T$. Theorem 4.5 provides a sufficient condition on the relationship between p_S and p_T , in terms of the Kullback-Leibler divergence, so that a δ -safe transformation with respect to p_S is a δ' -safe transformation with respect to p_T .

Before we start with the proof, let us argue why it makes sense to set $\mathcal{X}_S = \mathcal{X}_T = \mathcal{X}$ and $\mathcal{Y}_S = \mathcal{Y}_T = \mathcal{Y}$, as it is assumed in Theorem 4.5, even when we have more then two classes. When it comes to \mathcal{X} , any pre-trained feature transformation comes with a fixed input dimension. Therefore, in order to apply a feature transformation one usually needs to modify the input vector. When dealing with images, this often means resizing the image, whether it is by scaling the image, or by adding white/black pixels. This is an injective process as long as we do not reduce the dimension, which is reasonable to assume as we usually use transformations trained on larger inputs. Therefore, instead of \mathcal{X}_S we can consider a probability distribution mapped through an injective map $g: \mathcal{X}_S \rightarrow \mathcal{X}$, which is a safe transformation. We will omit the mention of g for the ease of notation. For \mathcal{Y} , we first assume that $\mathcal{Y}_T \subseteq \mathcal{Y}_S$, since we want to use feature transformations that work well on more difficult tasks. When f_S is safe with respect to p_S on $\mathcal{X}_S \times \mathcal{Y}_S$, it is easy to see that f_S is also safe with respect to the restriction of p_S to $\mathcal{X}_S \times \mathcal{Y}_T$. This does not necessarily hold when we weaken the condition to δ -safe. In that case, our assumption is that f is δ -safe with respect to p_S on $\mathcal{X}_S \times \mathcal{Y}_T$ in the first place, thus taking \mathcal{Y}_T as the source \mathcal{Y} .

PROOF OF THEOREM 4.5: Note that

$$R_{f(X_T)}^* - R_{X_T}^* \leq \underbrace{\left| R_{f(X_T)}^* - R_{f(X_S)}^* \right|}_{I_1} + \underbrace{\left| R_{f(X_S)}^* - R_{X_S}^* \right|}_{I_2} + \underbrace{\left| R_{X_S}^* - R_{X_T}^* \right|}_{I_3}.$$

Since f is δ -safe with respect to p_S , we have $I_2 \leq \delta$.

For I_1 , let $\tilde{p}_S := p_{f^{-1}}^{(S)}$ and $\tilde{p}_T := p_{f^{-1}}^{(T)}$ denote the corresponding measures with respect to $\tilde{\mathcal{X}}$, and let

$$y_{\tilde{x}}^{(S)} = \arg \max_{y \in \mathcal{Y}} \tilde{p}_S(\tilde{x}, y), \quad y_{\tilde{x}}^{(T)} = \arg \max_{y \in \mathcal{Y}} \tilde{p}_T(\tilde{x}, y).$$

For a fixed \tilde{x} we can assume without loss of generality that $\tilde{p}_S(\tilde{x}, y_{\tilde{x}}^{(S)}) \geq \tilde{p}_T(\tilde{x}, y_{\tilde{x}}^{(T)})$. Then

$$\begin{aligned} \left| \max_{y \in \mathcal{Y}} \tilde{p}_S(\tilde{x}, y) - \max_{y \in \mathcal{Y}} \tilde{p}_T(\tilde{x}, y) \right| &= \tilde{p}_S(\tilde{x}, y_{\tilde{x}}^{(S)}) - \tilde{p}_T(\tilde{x}, y_{\tilde{x}}^{(T)}) \\ &\leq \tilde{p}_S(\tilde{x}, y_{\tilde{x}}^{(S)}) - \tilde{p}_T(\tilde{x}, y_{\tilde{x}}^{(S)}) \\ &\leq \sum_{y \in \mathcal{Y}} |\tilde{p}_S(\tilde{x}, y) - \tilde{p}_T(\tilde{x}, y)|. \end{aligned}$$

Summing the above over all $\tilde{x} \in \tilde{\mathcal{X}}$ yields

$$\begin{aligned} I_1 &= \left| \sum_{\tilde{x} \in \tilde{\mathcal{X}}} \left[\max_{y \in \mathcal{Y}} \tilde{p}_S(\tilde{x}, y) - \max_{y \in \mathcal{Y}} \tilde{p}_T(\tilde{x}, y) \right] \right| \\ &\leq \sum_{\tilde{x} \in \tilde{\mathcal{X}}} \sum_{y \in \mathcal{Y}} |\tilde{p}_S(\tilde{x}, y) - \tilde{p}_T(\tilde{x}, y)| \\ &\stackrel{\Delta}{\leq} \sum_{\tilde{x} \in \tilde{\mathcal{X}}} \sum_{y \in \mathcal{Y}} \sum_{x \in f^{-1}(\tilde{x})} |p_S(x, y) - p_T(x, y)| \\ &= \sum_{x \in \mathcal{X}} \sum_{y \in \mathcal{Y}} |p_S(x, y) - p_T(x, y)| = \|p_S - p_T\|_1. \end{aligned}$$

Repeating the same calculation for I_3 implies $I_3 \leq \|p_S - p_T\|_1$. Combining the bounds for I_1, I_2 and I_3 yields

$$R_{f(X_T)}^* - R_{X_T}^* \leq \delta + 2\|p_S - p_T\|_1.$$

As in the previous section, Pinsker's inequality implies

$$R_{f(X_T)}^* - R_{X_T}^* \leq \delta + 2\sqrt{(2\ln 2)D_{KL}(p_S \| p_T)} \leq \delta + \varepsilon,$$

concluding the proof. \square

A.1.1 Safety and the g -squared loss

In this section we provide a characterization of δ -safe functions in terms of the g -squared loss of f , by proving Theorem 4.6. Since this will serve as a connecting point between the rates of convergence of a kNN classifier and the safety of a transformation, from this point onwards we restrict ourselves to binary classification, assuming that $\mathcal{Y} = \{0, 1\}$.

We start by proving an auxiliary lemma that is used both in the proof of Theorem 4.6 and in the proof of Theorem 4.1, presented in the main body, which is the main result of Section 4. It states that the g -squared loss of f on X can only be reduced by performing a change of variables to the identity function acting on $f(X)$.

Lemma A.3. *For any function f , one has $\mathcal{L}_{g,f(X)}(id) \leq \mathcal{L}_{g,X}(f)$.*

PROOF: Let $\tilde{X} = f(X)$. Note that for a fixed $\tilde{x} \in \tilde{\mathcal{X}}$,

$$\eta_{f^{-1}(\tilde{x})} = p_{f^{-1}}(1|\tilde{x}) = p(1|X \in f^{-1}(\tilde{x})) = \frac{\mathbb{E}_X \eta(X) \mathbf{1}_{\{X \in f^{-1}(\tilde{x})\}}}{\mathbb{E}_X \mathbf{1}_{\{X \in f^{-1}(\tilde{x})\}}}.$$

Hence,

$$\begin{aligned} \mathcal{L}_{g,f(X)}(id) &= \mathbb{E}_{\tilde{x}} \left((g \circ id)(\tilde{X}) - \eta_{f^{-1}(\tilde{X})} \right)^2 \\ &= \mathbb{E}_{\tilde{X}} \left(g(\tilde{X}) - \frac{\mathbb{E}_X \eta(X) \mathbf{1}_{\{X \in f^{-1}(\tilde{X})\}}}{\mathbb{E}_X \mathbf{1}_{\{X \in f^{-1}(\tilde{X})\}}} \right)^2 \\ &= \mathbb{E}_{\tilde{X}} \left(\frac{\mathbb{E}_X ((g \circ f)(X) - \eta(X)) \mathbf{1}_{\{X \in f^{-1}(\tilde{X})\}}}{\mathbb{E}_X \mathbf{1}_{\{X \in f^{-1}(\tilde{X})\}}} \right)^2, \end{aligned}$$

since for all $x, x' \in f^{-1}(\tilde{x})$ one has $(g \circ f)(x) = (g \circ f)(x') = g(\tilde{x})$. The Cauchy-Schwarz inequality yields

$$\begin{aligned} \mathcal{L}_{g,f(X)}(id) &\leq \mathbb{E}_{\tilde{X}} \frac{\mathbb{E}_X ((g \circ f)(X) - \eta(X))^2 \mathbf{1}_{\{X \in f^{-1}(\tilde{X})\}}}{\mathbb{E}_X \mathbf{1}_{\{X \in f^{-1}(\tilde{X})\}}} \\ &= \mathbb{E}_X ((g \circ f)(X) - \eta(X))^2 = \mathcal{L}_{g,X}(f), \end{aligned}$$

proving the claim. \square

We conclude this section by proving Theorem 4.6, the final ingredient for connecting the convergence rates of a kNN classifier with the Bayes error in the original space.

PROOF OF THEOREM 4.6: As in the proof of Lemma 4.3, we know that

$$\Delta_{f,X}^* \leq \mathbb{E}_X (p(y_x | x) - p_{f^{-1}}(y_x | f(x))) \leq \mathbb{E}_X |\eta(X) - \eta_{f^{-1}}(f(X))|.$$

The triangle and the Cauchy-Schwarz inequality, once for each term, yield

$$\begin{aligned} \Delta_{f,X}^* &\leq \mathbb{E}_X |\eta(X) - (g \circ f)(X)| + \mathbb{E}_X |(g \circ f)(X) - \eta_{f^{-1}}(f(X))| \\ &= \mathbb{E}_X |\eta(X) - (g \circ f)(X)| + \mathbb{E}_{\tilde{X}} |g(\tilde{X}) - \eta_{f^{-1}(\tilde{X})}| \\ &\leq \underbrace{(\mathbb{E}_X |\eta(X) - (g \circ f)(X)|^2)^{1/2}}_{\mathcal{L}_{g,X}(f)} + \underbrace{(\mathbb{E}_{\tilde{X}} |g(\tilde{X}) - \eta_{f^{-1}(\tilde{X})}|^2)^{1/2}}_{\mathcal{L}_{g,f(X)}(id)}. \end{aligned}$$

The claim now follows by Lemma A.3. \square

A.2 Convergence Rates of a kNN Classifier over Transformed Features

We now present the proof of Theorem 4.8, mimicking the proof of Theorem 6.2 from [18]. We insert our (weaker) probabilistic Lipschitz assumption where appropriate. It allows us to remove any additional constraint on f , leaving us with a statement dependent only on $\mathcal{L}_{g,X}(f)$. As discussed in Section 5, for $g(x) = \text{softmax}(W^T x + b)$ this can be used to rank various transformations f by simply reporting the mean squared error of the test set, denoted by $MSE_g(f, W, b)$. The price we need to pay is an additional additive error term. However, since an unavoidable error term as a function of $\mathcal{L}_{g,X}(f)$ already exists in Theorem 4.6, we accept it here, having in mind the flexibility it gives us. Optimizing this additive error term could form an interesting path for further research.

PROOF OF THEOREM 4.8: It is well known (see Chapter 1 in [18]) that

$$\mathbb{E}_n[(R_X)_{n,k}] - R_X^* \leq 2\mathbb{E}_n \mathbb{E}_X |\eta_{n,k}(X) - \eta(X)| \leq 2\sqrt{\mathbb{E}_n \mathbb{E}_X |\eta_{n,k}(X) - \eta(X)|^2}, \quad (\text{A.3})$$

where the last inequality is a simple application of the Cauchy-Schwarz inequality. With the assumptions as above, it suffices to prove that for all $w \in \mathbb{R}^d$,

$$\mathbb{E}_n \mathbb{E}_X |\eta_{n,k}(X) - \eta(X)|^2 \leq \frac{1}{k} + cL \left(\frac{k}{n}\right)^{2/d} + \delta + 2\varepsilon^2, \quad (\text{A.4})$$

for some $c > 0$. Let $(X_1, Y_1), \dots, (X_n, Y_n)$ be the set of n -samples distributed using $p(x, y)$. For $x \in \mathcal{X}$, let $n(i, x)$ denote the index of the i -th nearest neighbor of x in X_1, \dots, X_n . Then

$$\mathbb{E}_n |\eta_{n,k}(x) - \eta(x)|^2 = \underbrace{\mathbb{E}_n \left| \eta_{n,k}(x) - \frac{1}{k} \sum_{i \in [k]} \eta(X_{n(i,x)}) \right|^2}_{J_1(x)} + \underbrace{\mathbb{E}_n \left| \frac{1}{k} \sum_{i \in [k]} \eta(X_{n(i,x)}) - \eta(x) \right|^2}_{J_2(x)}.$$

For $J_1(x)$ note that

$$J_1(x) = \mathbb{E}_n \left| \frac{1}{k} \sum_{i \in [k]} (\eta_{n,k}(x) - \eta(X_{n(i,x)})) \right|^2 = \frac{1}{k^2} \sum_{i \in [k]} \mathbb{E}_n |\eta_{n,k}(x) - \eta(X_{n(i,x)})|^2 \leq \frac{1}{k}. \quad (\text{A.5})$$

For $J_2(x)$ we have

$$\mathbb{E}_X J_2(X) = \mathbb{E}_X \mathbb{E}_n \left| \frac{1}{k} \sum_{i \in [k]} (\eta(X_{n(i,X)}) - \eta(X)) \right|^2 \leq \frac{1}{k} \sum_{i \in [k]} \mathbb{E}_n \mathbb{E}_X |\eta(X_{n(i,X)}) - \eta(X)|^2,$$

by the Cauchy-Schwarz inequality. Let $\text{GOOD}_{\varepsilon,L} := \{(X, X') : |\eta(X) - \eta(X')| \leq \varepsilon + L\|X - X'\|\}$. Since η is (ε, δ, L) -probably Lipschitz and $(a+b)^2 \leq 2a^2 + 2b^2$, we have that

$$\begin{aligned} \mathbb{E}_X J_2(X) &\leq \frac{1}{k} \sum_{i \in [k]} \mathbb{E}_n (1 - \mathbb{P}((X, X_{n(i,X)}) \in \text{GOOD}_{\varepsilon,L})) + \frac{1}{k} \sum_{i \in [k]} \mathbb{E}_n \mathbb{E}_X (2\varepsilon^2 + 2L^2\|X_{n(i,X)} - X\|^2) \\ &\leq \delta + 2\varepsilon^2 + 2L^2 \underbrace{\mathbb{E}_X \mathbb{E}_n \frac{1}{k} \sum_{i \in [k]} \|X_{n(i,X)} - X\|^2}_{J_3(X)}. \end{aligned}$$

The term $J_3(X)$ is exactly the same as the upper bound for $I_2(X)$ in the proof of Theorem 6.2 in [18], where it is shown that there exists a $c > 0$ such that $\mathbb{E}_X J_3(X) \leq c(k/n)^{2/d}$.

Combining the bounds for J_1 , J_2 and J_3 proves the claim. \square

The final result of this section establishes the probabilistic Lipschitz condition in terms of the g -squared error of f . It is the glue that brings all the pieces together, having in mind that it is applied on $f(X)$.

PROOF OF LEMMA 4.9: Note that the triangle inequality implies

$$|\eta(X) - \eta(X')| \leq \underbrace{|\eta(X) - g(X)|}_{I_1(X)} + \underbrace{|g(X) - g(X')|}_{I_2} + \underbrace{|g(X') - \eta(X')|}_{I_1(X')}.$$

For I_2 note that the fact that g is L -Lipschitz implies $I_2(X, X') \leq L\|X - X'\|$.

For $I_1(X), I_1(X')$ we start by defining $\text{GOOD}_t := \{x \in \mathcal{X} : |\eta(x) - g(x)| \leq t\}$. Note that Markov's inequality yields

$$\mathbb{P}(X \notin \text{GOOD}_t) = \mathbb{P}(|\eta(X) - g(X)|^2 \geq t^2) \leq \frac{\mathcal{L}_{g,X}(id)}{t^2}.$$

Therefore,

$$\begin{aligned} \mathbb{P}(|\eta(X) - \eta(X')| \leq \varepsilon + L\|X - X'\|) &\geq \mathbb{P}(X, X' \in \text{GOOD}_{\varepsilon/2}) \\ &\geq \left(1 - \frac{4\mathcal{L}_{g,X}(id)}{\varepsilon^2}\right)^2 \geq 1 - \frac{8\mathcal{L}_{g,X}(id)}{\varepsilon^2}, \end{aligned}$$

concluding the proof. \square

B Extended Experimental Evaluation

As described in the main body of the paper, in this section we report additional experiments and outline the full experimental setup.

B.1 Experimental Setup

Feature Transformations. We provide the list of all tested feature transformations, together with their dimensionality, for the vision datasets and text classification datasets in Tables 2 and 3, respectively. We were not able to export the BOW (and hence neither the BOW-TFIDF nor the PCA transformed) feature representations for YELP due to the large amount of samples and their high dimensionality. Additionally, calculating the NCA representations did not successfully terminate for any of the text classification datasets, as this method does not scale to high dimensional and large-sample-size inputs. All reported transformations are publicly available through either the scikit-learn toolkit⁵, TensorFlow Hub⁶ or PyTorch Hub⁷.

Datasets. We use the standard splits provided by the datasets, as given in Table 1 in the main body. We collected all the datasets but YELP from the Tensorflow Datasets collection⁸, whereas YELP can be downloaded from <https://www.yelp.com/dataset>.

kNN Classifier. In order to illustrate the convergence rates, we subsample the training samples 10 times linearly (decreasingly), and perform 30 independent runs in order to report the variance. We plot the 95% confidence intervals on all the convergence graphs.

Logistic Regression Classifier. We train all the logistic regression models (on all the datasets and transformations mentioned earlier) using SGD with a momentum value of 0.9 and a batch size of 64 on the entire training set for 200 epochs, minimizing the cross entropy loss. We report the best achieved test set error (misclassification error) and mean squared error (MSE) using different values of L_2 regularizer (0.0, 0.0001, 0.001, 0.01, 0.1) and initial learning rates (0.0001, 0.001, 0.01, 0.1). We pre-process the input before training by normalizing the features to range between -1 and 1.

Training infrastructure. Training of the logistic regression models and evaluating kNN was executed on a single NVIDIA Titan Xp GPU.

⁵<https://scikit-learn.org/stable/>

⁶<https://tfhub.dev/>

⁷<https://pytorch.org/hub/>

⁸<https://www.tensorflow.org/datasets/>

Table 2: Feature transformations for images as features.

Transformation	Source	MNIST	CIFAR10	CIFAR100
<i>Identity - Raw</i>	-	✓	✓	✓
PCA (d=32)	scikit-learn	✓	✓	✓
PCA (d=64)	scikit-learn	✓	✓	✓
PCA (d=128)	scikit-learn	✓	✓	✓
NCA (d=64)	scikit-learn	✓	✓	✓
AlexNet(d=4096)	PyTorch-Hub	✓	✓	✓
GoogleNet (d=1024)	PyTorch-Hub	✓	✓	✓
VGG16 (d=4096)	PyTorch-Hub	✓	✓	✓
VGG19 (d=4096)	PyTorch-Hub	✓	✓	✓
ResNet50-V2 (d=2048)	TF-Hub	✓	✓	✓
ResNet101-V2 (d=2048)	TF-Hub	✓	✓	✓
ResNet152-V2 (d=2048)	TF-Hub	✓	✓	✓
InceptionV3 (d=2048)	TF-Hub	✓	✓	✓
EfficientNet-B0 (d=1280)	TF-Hub	✓	✓	✓
EfficientNet-B1 (d=1280)	TF-Hub	✓	✓	✓
EfficientNet-B2 (d=1408)	TF-Hub	✓	✓	✓
EfficientNet-B3 (d=1536)	TF-Hub	✓	✓	✓
EfficientNet-B4 (d=1792)	TF-Hub	✓	✓	✓
EfficientNet-B5 (d=2048)	TF-Hub	✓	✓	✓
EfficientNet-B6 (d=2304)	TF-Hub	✓	✓	✓
EfficientNet-B7 (d=2560)	TF-Hub	✓	✓	✓

Table 3: Feature transformations for natural language as features.

Transformation	Source	IMDB	SST2	YELP
<i>Identity - BOW</i>	-	✓	✓	✗
BOW-TFIDF	scikit-learn	✓	✓	✗
PCA (d=8)	scikit-learn	✓	✓	✗
PCA (d=16)	scikit-learn	✓	✓	✗
PCA (d=32)	scikit-learn	✓	✓	✗
PCA (d=64)	scikit-learn	✓	✓	✗
PCA (d=128)	scikit-learn	✓	✓	✗
ELMO (d=1024)	TF-Hub	✓	✓	✓
NNLM-EN (d=50)	TF-Hub	✓	✓	✓
NNLM-EN-WITH-NORMALIZATION (d=50)	TF-Hub	✓	✓	✓
NNLM-EN (d=128)	TF-Hub	✓	✓	✓
NNLM-EN-WITH-NORMALIZATION (d=128)	TF-Hub	✓	✓	✓
Universal Sentence Encoder (USE) (d=512)	TF-Hub	✓	✓	✓
BERT-Base (d=678)	PyTorch-Hub	✓	✓	✓

B.2 Convergence Plots

We provide convergence plots for an interesting subset of the datasets (CIFAR100 and IMDB) and transformations in Figures 5 and 6. From the results and scripts that we made available through the supplementary materials, one could simply create and analyze the plots for arbitrary combination of considered datasets and transformations. We remark that on both plots the transformations that achieve the best possible convergence in the finite sample regime do not have the lowest dimension. Furthermore, the starting point of the convergence lines for such transformations is typically much lower than the starting point of standard dimension-reduction techniques such as PCA. Having access to much more (ideally infinitely many) training samples would result in every line converging to the final, irreducible-bias term per transformation.

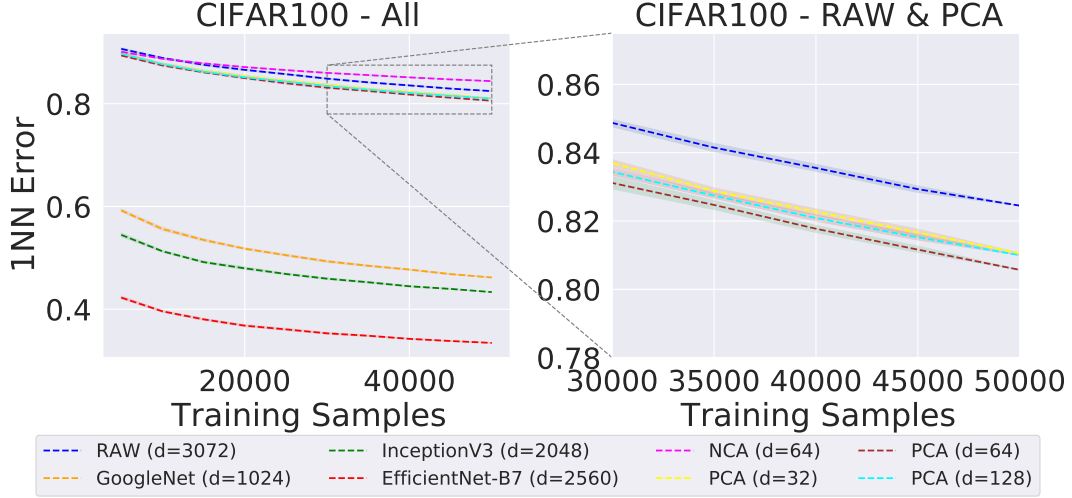


Figure 5: Impact of the dimension on CIFAR100 using all involved transformations (**Left**), and PCA-based transformation only (**Right**).

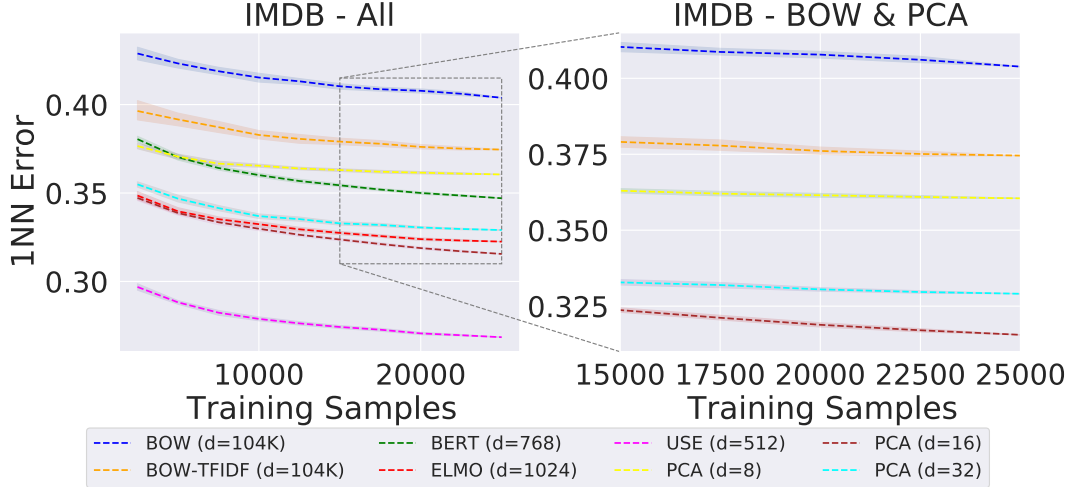


Figure 6: Impact of the dimension on IMDB using all involved transformations (**Left**), and PCA-based transformation only (**Right**).

B.3 On the Impact of the Hyper-Parameter k

It is well known that one can choose the hyper-parameter k to reach the best possible convergence in the finite data regime depending on the dataset. We investigate this with respect to transformations by showing that different transformations on the same dataset might have different optimal choices for k . This tradeoff for a fixed dataset is not clearly visible in the main Theorem 4.1 due to the usage of $\mathcal{O}(\cdot)$ notation, hiding the constants. However, by exploring the proof outline and analyzing (A.5), one realizes that the upper bound of J_1 is dependent on the posterior in the transformed feature space, which might change for a fixed input dataset. We report the empirically observed minimal kNN test error for values of k ranging from 1 to 250 in Table 4, for all the feature transformations on the computer vision datasets, and in Table 5, for the all the text classification datasets. In practice, when using kNN, one would take a portion of the training set as a validation set to choose the best hyper-parameter value for k and run an evaluation of the test set in order to control overfitting.

Table 4: Minimal kNN errors for the computer vision datasets.

Transformation	MNIST	CIFAR10	CIFAR100
<i>Identity - Raw</i>	0.029 (k=3)	0.646 (k=1)	0.825 (k=1)
PCA (d=32)	0.025 (k=8)	0.575 (k=16)	0.811 (k=1)
PCA (d=64)	0.025 (k=3)	0.601 (k=18)	0.806 (k=1)
PCA (d=128)	0.028 (k=3)	0.619 (k=1)	0.810 (k=1)
NCA (d=64)	0.026 (k=5)	0.600 (k=18)	0.837 (k=39)
AlexNet	0.165 (k=13)	0.244 (k=13)	0.509 (k=19)
GoogleNet	0.113 (k=9)	0.171 (k=10)	0.431 (k=18)
VGG16	0.133 (k=16)	0.208 (k=19)	0.476 (k=15)
VGG19	0.138 (k=15)	0.205 (k=19)	0.470 (k=16)
ResNet50-V2	0.092 (k=5)	0.152 (k=9)	0.397 (k=17)
ResNet101-V2	0.092 (k=6)	0.126 (k=9)	0.371 (k=10)
ResNet152-V2	0.094 (k=3)	0.137 (k=6)	0.373 (k=14)
InceptionV3	0.049 (k=13)	0.150 (k=10)	0.407 (k=17)
EfficientNet-B0	0.535 (k=7)	0.159 (k=9)	0.410 (k=17)
EfficientNet-B1	0.691 (k=7)	0.125 (k=7)	0.368 (k=24)
EfficientNet-B2	0.630 (k=8)	0.120 (k=10)	0.352 (k=10)
EfficientNet-B3	0.789 (k=7)	0.090 (k=6)	0.312 (k=13)
EfficientNet-B4	0.745 (k=25)	0.085 (k=7)	0.307 (k=13)
EfficientNet-B5	0.804 (k=23)	0.092 (k=8)	0.317 (k=12)
EfficientNet-B6	0.649 (k=25)	0.092 (k=6)	0.326 (k=10)
EfficientNet-B7	0.543 (k=14)	0.087 (k=12)	0.316 (k=9)

Table 5: Minimal kNN errors for the text classification datasets.

Transformation	IMDB	SST2	YELP
<i>Identity - BOW</i>	0.334 (k=36)	0.349 (k=6)	-
BOW-TFIDF	0.243 (k=247)	0.249 (k=26)	-
PCA (d=8)	0.274 (k=155)	0.408 (k=81)	-
PCA (d=16)	0.226 (k=159)	0.382 (k=236)	-
PCA (d=32)	0.216 (k=175)	0.375 (k=174)	-
PCA (d=64)	0.228 (k=157)	0.377 (k=147)	-
PCA (d=128)	0.241 (k=196)	0.374 (k=170)	-
ELMO	0.255 (k=37)	0.195 (k=206)	0.424 (k=166)
NNLM (d=50)	0.287 (k=77)	0.294 (k=227)	0.475 (k=86)
NNLM (d=128)	0.255 (k=57)	0.241 (k=148)	0.452 (k=43)
NNLM (d=50, w/ normalize)	0.259 (k=45)	0.288 (k=36)	0.455 (k=92)
NNLM (d=128, w/ normalize)	0.227 (k=47)	0.241 (k=162)	0.427 (k=45)
Universal Sentence Encoder (USE)	0.188 (k=183)	0.201 (k=186)	0.387 (k=75)
BERT-Base	0.266 (k=45)	0.267 (k=8)	0.441 (k=51)